

## Article

# Sustainable Measures for Mitigation of Flooding Hazards: A Case Study in Shanghai, China

Yao Yuan <sup>1,2</sup>, Ye-Shuang Xu <sup>1,2,\*</sup> and Arul Arulrajah <sup>3</sup>

<sup>1</sup> State Key Laboratory of Ocean Engineering, School of Naval Architecture, Ocean, and Civil Engineering, Shanghai Jiao Tong University, Shanghai 200240, China; yuanyao12@sjtu.edu.cn

<sup>2</sup> Collaborative Innovation Center for Advanced Ship and Deep-Sea Exploration (CISSE), Shanghai Jiao Tong University, Shanghai 200240, China

<sup>3</sup> Department of Civil and Construction Engineering, Swinburne University of Technology, Melbourne, VIC 3122, Australia; aarulrajah@swin.edu.au

\* Correspondence: xuyeshuang@sjtu.edu.cn; Tel.: +86-21-3420-4301

Academic Editors: Franco Salerno and Athanasios Loukas

Received: 23 February 2017; Accepted: 25 April 2017; Published: 28 April 2017

**Abstract:** Global warming induces temperature variations and sea level changes for a long period of time. Many coastal cities around the world have experienced the harmful consequences of sea level changes and temperature variations. The city of Shanghai in China also suffers from the serious consequences of these two climatic factors. The geological and climatic conditions of Shanghai make it sensitive to flooding risks during heavy rainfall events. This paper analyses the conditions of sea level changes, temperature variations, and heavy rainfall events in Shanghai. Correspondingly, eustatic sea level change, tectonic movement of the continent, and land subsidence in Shanghai have effects on sea level changes. Correlation analysis indicates extraordinary short duration rainfall events have a relationship with temperature variations due to global warming. Moreover, the number of extraordinary torrential rainfall events also has a correlation with sea level changes. Pluvial flooding and potential damage to coastal structures are more likely to have serious effects as the number of flooding hazard events due to global warming and sea level changes increases. This study also established that to efficiently protect the environment, control economic losses, and prevent potential hazards, extra countermeasures including monitoring, forecasting, and engineering technology treatment should be adopted. Monitoring measurements combined with a database system on a website was found to be useful for forecasting and simulating flooding hazards. For systematic sustainable urban water system management, appropriate treatment technologies, such as sustainable urban water system, which can control and manage water quantity and quality, namely “the Sponge City”, should also be considered.

**Keywords:** global warming; sea level variations; torrential rainfalls; flooding hazards; Shanghai

## 1. Introduction

In recent decades, global warming, which is a mix of rising temperatures and unstable climate, has been an important issue in the research of environmental changes. Research indicates that the presence of greenhouse gases in the atmosphere and human activities are the main contributing factors that cause global warming [1,2]. Numerous coastal mega-cities around the world have experienced hazards due to global warming. These hazards include increased demand for groundwater due to temperature rise [3–6], ocean acidification, and the collapse of ecosystems worldwide on land and at sea [7–10]. Moreover, rising temperatures and rising sea levels due to global warming tend to increase the probability of heavy rainfall risks, particularly in coastal cities [11,12]. The increase in the number of intensive precipitation events will also increase the potential risks for pluvial flooding resulting in

the endangerment of urban safety. China has a coast line that extends over a distance of 18 thousand kilometers. Sustainable economic and social development of many coastal cities in China has been endangered by the adverse effects of global warming that include typhoons and pluvial flooding.

Shanghai is located on the south bank of the Yangtze River, bordered to the east by the East China Sea, and is one of the largest coastal cities in the world, occupying an area of 6340 km<sup>2</sup> [13,14]. The geological profile of this city is mostly composed of soft deltaic deposit [15–18]. The Huangpu River, a tributary of the Yangtze River, runs through Shanghai. Figure 1 presents a schematic of the Shanghai administrative region [19–23]. The annual rainfall is approximately 1200 mm, of which 60% falls during the flooding season from May to September [24–27]. The first month of the flooding season (the month of May) is usually referred to as the ‘Meiyu period’, in which rainfall events last for several days. Since the 1980s, Shanghai has constructed numerous drainage systems, such as water sluices and drainage pumps; however, high precipitation still leads to pluvial flooding events, which result in huge economic losses, and furthermore endanger urban safety. Global warming brings about more extreme storms, such as typhoons, which frequently increase the flood hazard level. For example, Typhoon Canhong in 2015, which landed in Zhejiang province, resulted in economic losses totaling 1.98 billion RMB (about 300 million USD) [28]. Rainfall-runoff due to typhoons caused more than ten thousand buildings to be inundated. Thus, it is necessary to analyze the effects of global warming with respect to flooding risks and to propose appropriate countermeasures to cope with the impact of global warming.

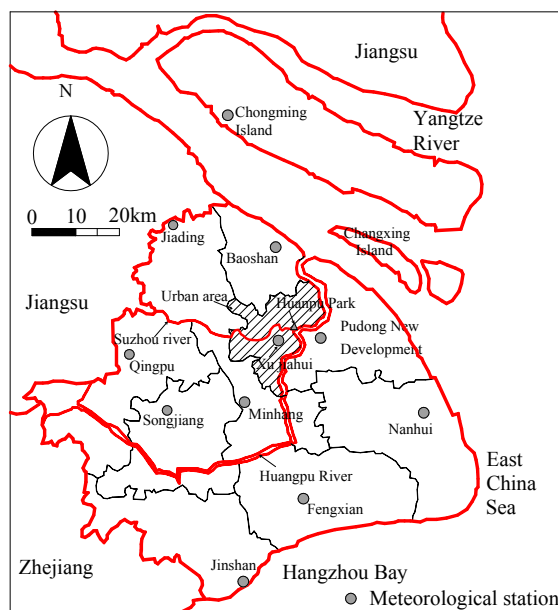


**Figure 1.** Schematic view of Shanghai depicting the locations of the meteorological stations.

At present, Shanghai’s elevation ranges from 2.2 to 4.5 m above the mean sea level [29], with some central parts of the urban area being lower than 3 m [29,30]. Based on the China Ocean Bulletin [31], the eustatic sea level in Shanghai has increased by 115 mm over the past thirty years. In addition, continental tectonic movement and human activities such as groundwater withdrawal [32–35], pipe jacking constructions [36–38], deep excavations [39–42] and tunnel constructions [43,44] tend to induce the land subsidence and have an effect on the relative sea level. Due to the low elevation of Shanghai, pluvial flooding events are more likely to occur with relative sea level rises. It is therefore increasingly urgent to provide appropriate countermeasures to control relative sea level changes induced by global warming.

The objectives of this paper are to: (i) discuss the correlation between heavy rainfall events and associated factors, namely, sea level changes and temperature variations induced by global

warming; (ii) discuss hazards that arise due to heavy rainfall events; and (iii) propose appropriate countermeasures against flooding hazards.

## 2. Methodology and Study Area

### 2.1. Methodology

The methodological approach adopted in this study comprises the combination of analyses of database repositories on temperature, sea level and frequency of torrential rainfalls in Shanghai over the past thirty years, as well as a series of correlation analysis of torrential rainfalls and temperature or sea level variations due to global warming. Sea level data are published as the China Ocean Bulletin by the China Oceanic Administration (COA) and can be downloaded from the COA official website. More specifically, databases of temperature and the frequency of torrential rainfalls were meticulously gathered from meteorological stations and published papers, whereas the sea level elevations were systematically obtained from the website of China's oceanic administration. Besides considering these databases extend over a period of more than 30 years (up to the 1960s), the analysis approach adopted in this study differed with respect to the meteorological features considered. Thus, the annual average temperature at Xujiahui meteorological station was used for temperature, while the accumulative anomalies method was utilized for analysing the database of the frequencies of torrential rainfalls. By using the latter method, the five-year moving data of temperature and sea level were computed. Thereafter, the linear tendency estimate method was implemented to analyse correlations between sea level changes and the frequencies of heavy rainfall events.

### 2.2. Study Area and Scenario in Shanghai

The rainfall monitoring data for Shanghai are available dating back 130 years to 1873. Since 2005, Shanghai has had 55 rainfall measuring sites. After the monitoring data are collected at the precipitation sites, the data are sent to meteorological stations for rainfall forecasting. Figure 1 shows the location of meteorological stations in Shanghai. Generally, rainfall events are divided into four types [45]: (i) light rainfall (cumulative precipitation ( $p$ ) less than 10 mm/day ( $p < 10$  mm/day)); (ii) moderate rainfall ( $10 \leq p < 25$  mm/day); (iii) heavy rainfall ( $25 \leq p < 50$  mm/day); and (iv) torrential rainfall ( $p \geq 50$  mm/day). Torrential rainfalls in Shanghai are often intensely concentrated within a period of 12 h or less. Therefore, cumulative precipitation higher than 30 mm in 12 h (namely,  $p \geq 30$  mm/12 h) is defined as a torrential rainfall event in Shanghai [30,46]. In this paper, the definition for the duration time of heavy rainfall is as follows [46,47]: beginning with the first meteorological station rains, ending with the last meteorological station when rain stops, while the interval between the ending time of the first meteorological station and the beginning time of the last meteorological station is less than 3 h.

Based on the cumulative precipitation, torrential rainfall is divided into three stages: (i) weak torrential rainfall ( $30 \text{ mm}/12 \text{ h} \leq p \leq 59 \text{ mm}/12 \text{ h}$ ); (ii) moderate torrential rainfall ( $60 \leq p \leq 99 \text{ mm}/12 \text{ h}$ ); and (iii) extraordinary torrential rainfall ( $p \geq 100 \text{ mm}/12 \text{ h}$ ). Figure 2 shows the average values for five-year torrential rain frequencies in Shanghai during the period 1981 to 2010 [46]. The amount of torrential rainfall shows a stable trend, ranging from 18 to 23 occurrences per year from 1981 to 2010. However, different types of torrential rainfall have varying trends. The annual average number of moderate torrential rainfall and extraordinary torrential rainfall events from 1995 to 2010 increases by about 0.8 occurrences/year and 0.4 occurrences/year, respectively, compared with the period from 1980 to 1994, while the annual average number of weak torrential rainfall events from 1995 to 2010 decreases by about 2 occurrences/year (2 occurrences per year) compared with the period from 1980 to 1994. The duration of rainfall events ( $D_t$ ) is used to evaluate the torrential rain occurrences. With due consideration for the time duration, torrential rainfall events can be divided as follows: (i) extraordinarily long duration rainfall ( $D_t \geq 36$  h); (ii) long duration rainfall ( $24 \leq D_t < 36$  h); (iii) moderate duration rainfall ( $12 < D_t < 24$  h); (iv) short duration rainfall ( $6 < D_t < 12$  h); (v) extraordinarily short duration rainfall ( $D_t < 6$  h). The cumulative precipitation

should also exceed 30 mm during durations of short or extraordinarily short duration rainfalls. Torrential rainfalls will easily induce pluvial flooding hazards, but not all the torrential rainfall events will induce hazards. When the total precipitation is higher than the storage capacity of the drainage system, or the average precipitation in one hour is higher than the drainage capacity of the municipal drainage system, pluvial flooding tends to occur. The extraordinary torrential rainfall and extraordinarily short duration rainfall events are the two conditions that most likely result in pluvial flooding hazards, which will be discussed in the following analysis.

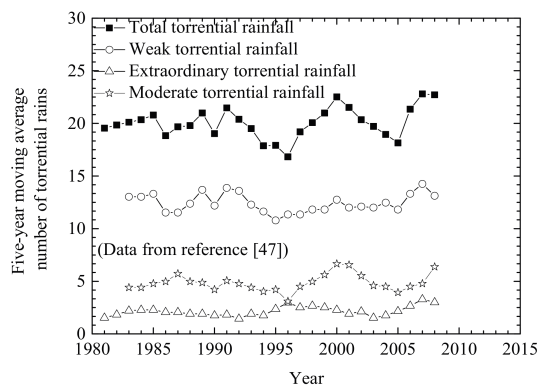


Figure 2. Average values of five-year torrential rain frequencies from 1980 to 2010.

### 3. Characteristics of Global Warming in Shanghai

#### 3.1. Temperature Variation

One remarkable characteristic of global warming is the increase in temperatures. Based on data from the National Aeronautics and Space Administration (NASA) Goddard Institute, the average temperature around the world has risen by 1.4 degrees since the 1880s. From the 1960s, the overall annual average temperature in China shows an evidently increasing trend, at a rate of  $0.25\text{ }^{\circ}\text{C}/10\text{ year}$ . Figure 3 shows the average temperature variation at the Xujiahui Station of Shanghai from 1960 to 2015 [48,49]. Before the 1980s, variations in the annual temperature fluctuated within a range of  $15\text{ }^{\circ}\text{C}$  to  $16.2\text{ }^{\circ}\text{C}$ . After the 1980s, the temperature increased markedly. The annual average temperature has risen by approximately  $3.5\text{ }^{\circ}\text{C}$  from 1980 to 2007. As shown in the figure, the rising rate of temperature variations in Shanghai is about  $0.61\text{ }^{\circ}\text{C}/10\text{ year}$ , while the highest annual average temperature was  $18.5\text{ }^{\circ}\text{C}$  in 2007. Subsequently, there was a minimal decrease in the average temperature. The change in temperature may decrease due to the southward cold air from the north of China, increasing the amount and frequency of excessive rainfall events in Shanghai. Moreover, due to global warming and urbanization, the aforementioned increase in temperature is more likely to cause potential risks, particularly massive pluvial flooding hazards.

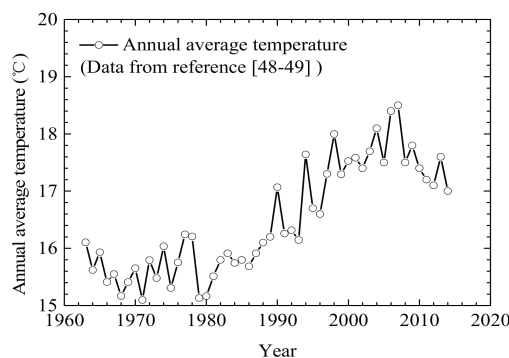
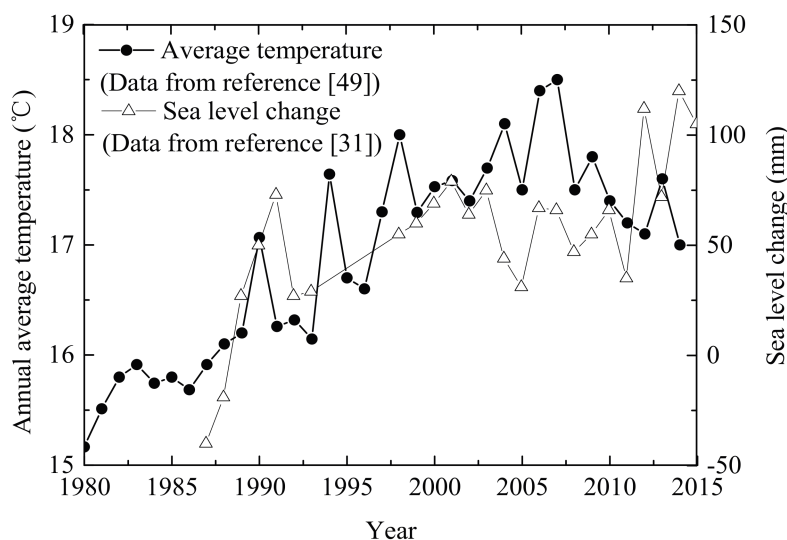


Figure 3. Temperature variation at the Xujiahui station of Shanghai from 1960 to 2015.



### 3.2. Sea Level Change

The main causes of sea level changes include heat content expansion of ocean water and exchange of water between the ocean and other reservoirs. Due to the lack of an open sea database, current sea level changes are mainly believed to be induced by global warming, which has contributed to rising sea levels over a long period of time [50]. Approximately 70% of eustatic sea level changes are expected to be induced by the heat content change of ocean water. Excluding the influence of crustal tectonic movement and land subsidence, satellite-based estimations suggest that the rate of global sea level change has been in the range of  $1.5 \pm 0.5$  mm/year over the past decade [50–54]. Based on the China Ocean Bulletin [31], the average annual rate of sea level rise was about 3.0 mm from 1980 to 2015, which is far higher than the global average sea level increasing rate. Figure 4 shows the sea level change and the annual average temperature variation in Shanghai. Internationally, the mean sea level is defined as the average sea level from 1975 to 1986 [31]. Before 2010, variations between the actual eustatic sea level and the mean sea level fluctuated within a range of 30 mm to 80 mm. After 2010, the eustatic sea level began to increase sharply. As shown in the figure, the highest sea level change on record reached 122 mm above the mean sea level in 2012. The annual average temperature variation and the sea level change have similar trends. In addition, continental tectonic movements have had an effect on sea level rise. The tectonic movement in Shanghai is approximately 1 mm/year [55]. Because of soft deltaic deposits, land subsidence due to human activity, such as urbanization and groundwater withdrawal, will decrease the height of sea flooding walls and is also an important factor affecting the sea level due to land surface changes. Figure 5 shows the annual land subsidence from 1921 to 2015 in Shanghai. Before 1960, the annual land subsidence increased sharply. After 1965, with some measures to reduce the land subsidence, such as reducing the net groundwater withdrawal volume, adjusting the main withdrawal layers and recharging the groundwater of the aquifer, the average annual land subsidence decreased to 3–10 mm/year [5,15]. Sea level changes due to the aforementioned factors as well as crustal tectonic movement and land subsidence are usually defined as relative sea level changes. The low elevation and relative sea level change in Shanghai result in high risk for pluvial flooding hazards along the coastal regions during heavy rainfall events.



**Figure 4.** Relationship between sea level change and annual average temperature variation in Shanghai.

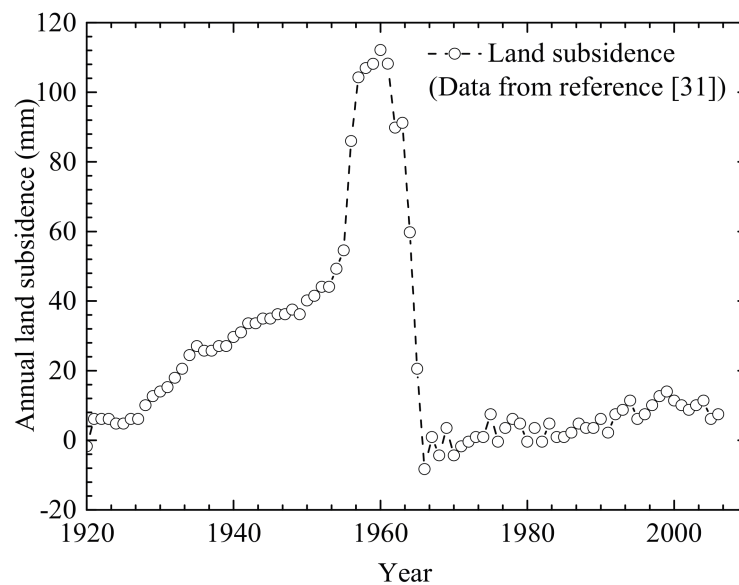


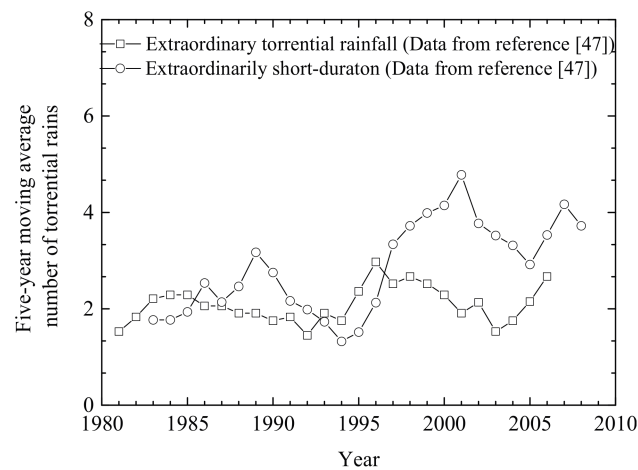
Figure 5. Annual land subsidence in Shanghai from 1920 to 2015.

#### 4. Pluvial Flooding Hazards in Shanghai

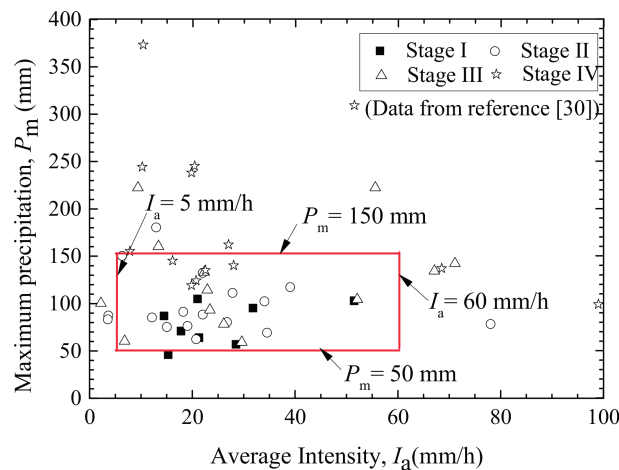
When heavy rainfall occurs, it will affect the daily lives of local residents, but not all torrential rainfall will result in catastrophic disasters. The two main factors affecting torrential rainfall are the maximum precipitation ( $P_m$ ) and the time duration ( $D_t$ ). Though  $D_t$  is very long and  $P_m$  is very large, abundant rainwater can be discharged to the drainage system in a timely manner. This type of heavy rainfall will, however, not induce effects such as the inundation of roads. Therefore, the parameters,  $P_m$ , and the average intensity,  $I_a$  ( $I_a = P_m/D_t$ ), namely the average hourly precipitation, were used to analyse pluvial flooding. The impact of pluvial flooding due to heavy rainfall was evaluated by considering the amount of inundated sections of road ( $N_R$ ). Table 1 depicts the impact levels of pluvial flooding, which are classified into four categories ranging from I to IV. Therefore, the extraordinary torrential rainfall and the extraordinarily short duration rainfall events more easily induce flooding hazards. Figure 6 shows the five-year moving average number of extraordinary torrential rainfalls and extraordinarily short duration rainfalls. As shown in Figure 6, the two types of rainfall events present an increasing trend since 1995. Figure 7 shows the relationship between  $I_a$  and  $P_m$  for 54 heavy rainfall events in Shanghai during the last fifteen years. In these rainfall events,  $P_m$  is mainly concentrated in the range from 50 mm to 150 mm, while  $I_a$  is within the range of 5 mm/h to 60 mm/h. If  $P_m$  is smaller than 50 mm or  $I_a$  is smaller than 5 mm/h, fewer pluvial flooding events will occur even with heavy rainfall (which would correspond to impact Stage I). However, if  $P_m$  is higher than 150 mm, or  $I_a$  is higher than 60 mm/h, the current capacity of pluvial flooding resistance in Shanghai cannot prevent a flooding event. For example,  $P_m$  and  $I_a$  of the pluvial flooding event on 25 August 2008 were 162 mm and 27 mm/h, respectively. More than 150 road sections ( $N_R > 150$ ) were inundated on 25 August 2008. It is therefore essential to improve the drainage system capacity in order to prevent this kind of pluvial flooding event (which would correspond to impact Level IV).

Table 1. Impact level of pluvial flooding event [30].

Impact Level	Number of Sections of Inundated Road Reported by Media
Level I	"A few" or $N_R \leq 3$
Level II	"Less than 10", "More than 10" or $4 \leq N_R \leq 11$
Level III	From "Less than 20" to "more than 40" or $12 \leq N_R \leq 50$
Level IV	From "More than 50" to "More than 200" or "Extensively water-logged" or $N_R \geq 51$



**Figure 6.** Five-year moving average number of extraordinary torrential rainfalls and extraordinarily short duration rainfalls.



**Figure 7.** Relationship between  $I_a$  and  $P_m$  in the rainfall events that caused pluvial flooding from 2001 to 2015.

## 5. Correlation between Heavy Rainfall and Global Warming

Studies of recent heavy rainfall events due to the temperature increase induced by global warming point to two main causes: (i) abundant water vapour and (ii) air cross-ventilation. Air temperature increases will lead to heat increases in the atmosphere and air cross-ventilation [47]. Because of the abundant water vapour in the atmosphere along the coastal area of Shanghai, the severe air cross-ventilation due to a temperature increase could increase the number of convective torrential rainfall events, especially during the Meiyu period. Global warming has an effect on the variation of the precipitation system. This potential increase in the aforementioned weather system due to global warming will induce warm-sector rainfall and further increase the frequency of extraordinarily short duration rainfall events. According to data from the eleven weather stations, Figure 8a depicts the variations of the five-year moving average temperature and five-year moving average number of extraordinarily short duration rainfall events from 1980 to 2010. Figure 8b shows the relationship between the five-year moving average number of extraordinarily short duration torrential rainfalls and the temperature variation. Despite the data being limited and scattered, the influence of the temperature is significant. With an increase in temperature, the frequency of extraordinarily short duration torrential rainfalls increases. As shown in Figure 8b, if the temperature increases by about 1 °C, the number of extraordinarily short duration torrential rainfall events increases to 0.87 occurrences.

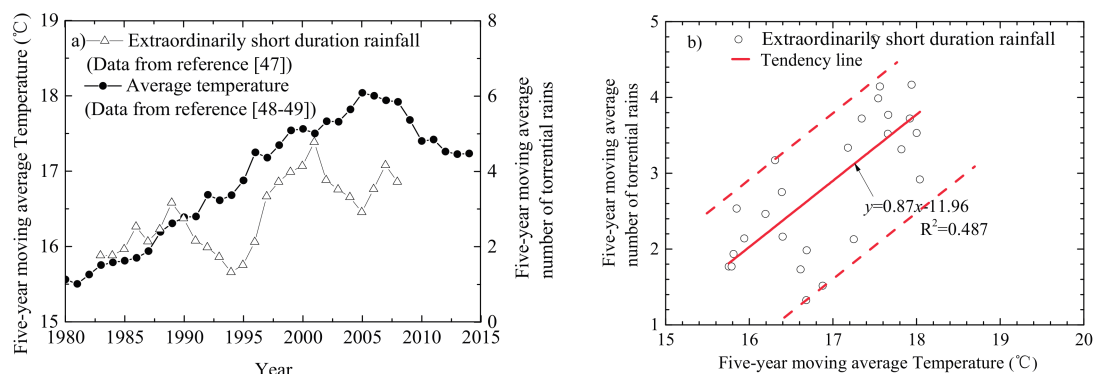


**Figure 8.** Relationship between five-year moving average temperature and five-year moving average number of extraordinarily short duration rainfall events. (a) Variations of temperature and rainfall events; (b) Relationship between temperature and rainfall events.

An alternative mechanism contributing to the frequent heavy rainfall events in Shanghai is associated with rising sea levels. The change in eustatic sea level due to global warming may have an effect on storm tides. Storm tides will affect the number and the intensity of heavy rainfall events and lead further to extraordinary torrential rainfall events. The observed results at eleven weather stations (Figure 9a) show the sea level change and the number of extraordinary torrential rainfalls. Figure 9b plots the relationship between the five-year moving average sea level change and the five-year moving average number of extraordinary torrential rainfall events. Similar to the effects of temperature, the number of occurrences of extraordinary torrential rainfall events tends to result in only a minimal increase with any corresponding increase in the average sea level. As shown in Figure 9b, if the sea level change increases by 10 mm, the number of the extraordinary torrential rainfalls tends to increase by 0.041 occurrences.

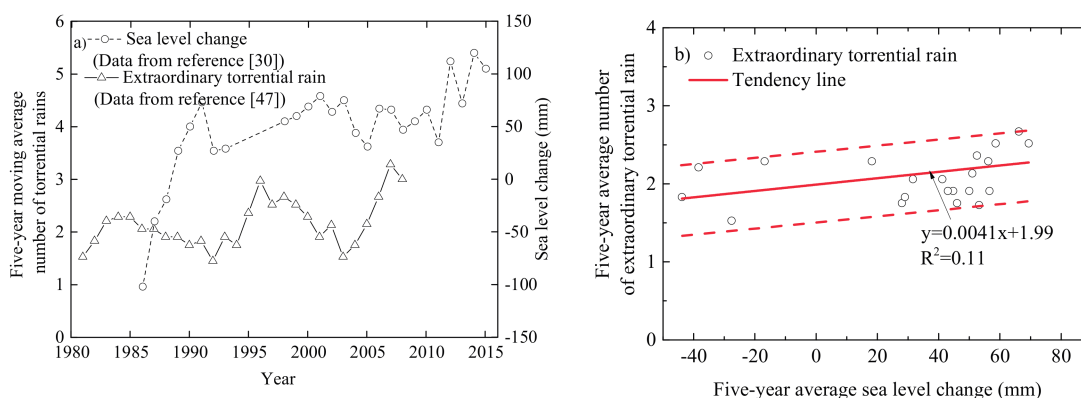


**Figure 9.** Relationship between the five-year moving average sea level change and the five-year moving average number of extraordinary torrential rainfalls (a) variations of sea level change and rainfall events; (b) relationship between temperature and rainfall events.

## 6. Potential Risks and Prevention Countermeasures Due to Pluvial Hazards

### 6.1. Potential Damage Due to Flooding Hazards

Many heavy rainfall events with precipitation levels higher than 50 mm/h have occurred in Shanghai recently. However, the existing drainage in the city can only withstand precipitation rates lower than 36 mm/h. Therefore, heavy rainfall events easily induce pluvial flooding hazards and result in flooded roads. Figure 10 shows the highest tide levels observed at Huangpu Park Station in the urban centre of Shanghai, the position of which is noted in Figure 1 [56]. The tides have shown

an increasing trend in the rise in river levels since the 1960s. Since the 1960s, the highest tides have all been above 4 m, which is higher than the ground elevation of most areas in Shanghai. Figure 11 shows a photograph of the floodwall along the Suzhou River, a tributary of the Huangpu River [57]. The floodwall was raised three times, and its height has now reached 6.9 m. The reason is that land subsidence along the Suzhou River has changed the relative sea level and impaired the defence ability of the flooding wall. Xu et al. (2012) [15] proposed that the cumulative land subsidence from 1921 to 2010 is more than 2 m in the urban area of Shanghai. With the increased rate of euastic sea level changes and land subsidence rates, the defence ability of the flood proof wall tends to be impaired, while the force of the surges will be enhanced and the maximum tide heights are likely to exceed the current height. Moreover, the sea level rise shortens the recurrence interval of the extreme high water level, and the sea water may easily overtop the breakwaters. This will change the ranking of the coastal defence structures, in terms of the magnitude of flooding which they can withstand. For example, the flood control wall in Shanghai has reduced in rank from protecting against a one-in-1000 year flood to protecting against a one-in-200 year flood. On the other hand, flooding hazards will disturb the freshwater ecosystem for local residents. When pluvial flooding occurs, the water in the Yangtze River and the Huangpu River may flow backwards into inland rivers and pollute fresh potable water. At present, 70% of fresh water supplies for Shanghai come from reservoirs and tributaries in the Yangtze estuary, and flooding hazards may pollute the water and lead to a shortage of fresh water supplies.

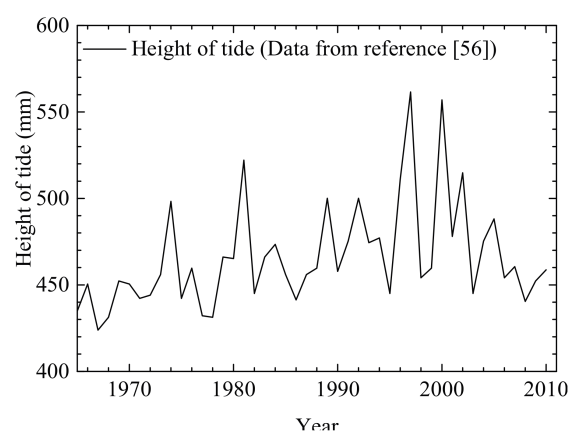


**Figure 10.** Maximum height of the tide.

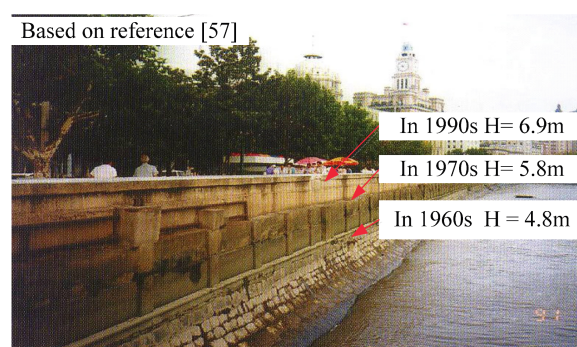


**Figure 11.** Photo of the floodwall along Suzhou River.

## 6.2. Monitoring for Flood Disaster Prevention: Current Status of Assessment

It is important to monitor temperature variations and sea level changes to forecast their potential risks, such as the pluvial flooding hazards in Shanghai. Nowadays, automatic monitoring systems such

as a Geographic Information System (GIS), a Global positioning system (GPS) and Remote Sensing (RS) have been adopted in risk assessment surveys [58–66]. For example, a methodology based on GPS has been developed for assessing vulnerability to sea-level rise and associated storm surges in Shanghai. An inundation analysis model using ArcGIS and ArcToolbox was established to assess the impact of sea level rise. The variables for sea-level rise, the DEM, the map of analysis factors, the boundary data and mean sea level input data were integrated into this model. With this model, the impact of sea level rise on analysis factors can be presented [57]. With the variety of data from RS, GIS for constructing topographic maps, and sea-level change data from the Intergovernmental Panel for Climate Change (IPCC), 40% of the terrestrial area of the Dongtan Reserve in Chongming Island of Shanghai will be flooded in 2100 with an estimated 0.88 m increase in the maximum sea level change [58].

The formation of torrential rainfall requires three main factors to occur; adequate water supply, strong vertical rise conditions and long rainfall duration. In order to predict torrential rainfalls, a rainfall forecast model is established based on satellite pictures, cloud cluster data, and other relevant information including air speed and temperature. Combining the rainfall forecast model and weather prediction, the torrential rainfalls can be forecast [63]. Because of the associated effects of atmospheric motion, different periods, and spatial scales, the accuracy of forecasting torrential rainfall, which is within 25% in the USA [67], is not high. Therefore, it is important to establish a digital heavy rainfall simulation model which can improve the forecasting accuracy in future research. Due to complicated factors caused by heavy rainfall, many studies have been conducted to investigate torrential rainfall. Cao et al. (2008) [68] utilized GPS/PWV images to investigate severe convective torrential rainfall that occurred in Shanghai on the 25th of August 2008 in order to develop rules for forecasting heavy rainfall. Fang et al. (2009) [69] introduced an early warning system for rainstorm water logging in Shanghai. On the basis of the WebGIS platform and with consideration of the geographical characteristics of Shanghai, the monitoring and forecasting rainstorm water logging system was developed. With this system, the real-time rainfall information and quantitative precipitation forecasting database were monitored. Based on the GIS platform, the multi-objective comprehensive management system for stormwater integrated management can simulate the ground runoff, analyse the rainfall and flooding submerged area and implement rainfall resource utilization. In this system, the Green Stormwater Infrastructure (GSI) is proposed to replace the traditional rainwater drainage, in which many infrastructures such as ecological parks and landscape areas are adopted to adjust the rainwater runoff and store the redundant rainwater for cyclic utilization [70]. For example, Xu et al. (2013) [71] proposed this kind of management system in Lingang New City, which is located in the southeast of Shanghai, for regional flooding control and rainfall utilization. With this integrated management system, the ground runoff, rainfall and flooding submerged area can be simulated and controlled.

### 6.3. Engineering Treatment Technology

In light of the characteristics of various potential risks in pluvial flooding hazards induced by temperature variations and sea level changes, different engineering treatment technologies should be adopted [72–78]. The main weather system induced torrential rainfalls in Shanghai is classified under one of the following categories: “the stationary front”, “warm sector”, “low pressure”, and “the typhoon” [47]. Shanghai is located in the high voltage or the low pressure trough of the warm sector. Convective precipitation induced by strong convergence and unstable thundershowers induced by cyclonic curvature often occur in the warm sector areas of Shanghai [46,47]. Due to the effects of global warming and the “urban heat island effect”, torrential rainfall induced by warm-sector weather systems has become increasingly severe. Therefore, new clean energy alternatives, for example, hydrogen and wind energy sources, can be adopted to decrease greenhouse gas emissions, slow down global warming, and reduce torrential rainfalls induced by the warm-sector weather system.

Increasing the water storage capacity and improvement of the drainage system are also used as countermeasures to help prevent pluvial flooding hazards due to torrential rainfalls. Due to the impacts of rapid urbanisation, sediment depositions, and deterioration due to siltation, the length



of rivers in Shanghai has decreased from the year 1843. The total length of Shanghai rivers is now approximately 24,915 km, and the total area of these rivers is 642.7 km<sup>2</sup> [77]. If countermeasures such as dredging sediment depositions, connecting and deepening the rivers are adopted, the water storage capacity can increase, thus mitigating pluvial flooding. For example, if the average depth of all the rivers increases by one meter, the water storage capacity can increase by 6.427 billion m<sup>3</sup>. Moreover, many pluvial flooding hazards due to extraordinary torrential rainfall occur in the underpasses due to the failure of the drainage system, as shown in Figure 12. This is due to the sewers under or nearby the underpasses that fail to discharge the water in a timely manner. If the discharge capacity of the drainage system is improved, for example, by cleaning up road gullies blocked by leaves or debris and maintaining damaged sewers to ensure the maximum performance of the sewage network, no further pluvial flooding will occur.

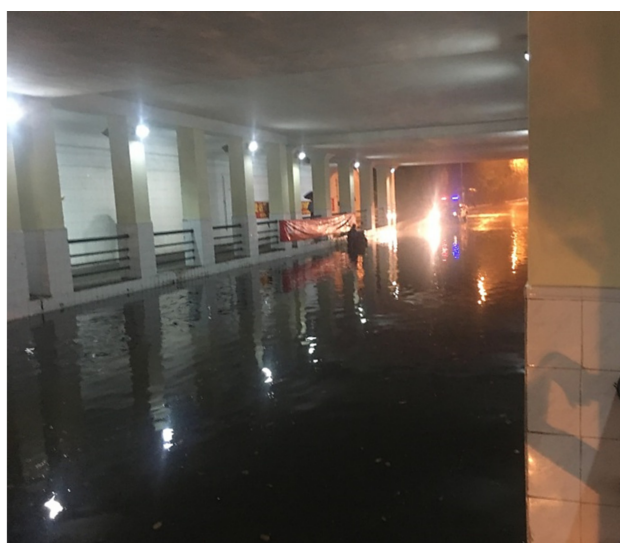


**Figure 12.** Photo of an underpass after short duration rainfall.

After a number of years of research in China on rainwater management, the “Sponge City” concept was put forward in 2013 and was then gradually accepted by the public [74]. It is a systemic sustainable urban water system, which can help control and manage water quantity and quality using various measures. With this system, excessive rainfall can be controlled and discharged in a timely manner. Figure 13 shows the schematic diagram of the Sponge City concept. When the precipitation is very low, the first stage can be turned on for discharging rainwater. As the precipitation increases, the other two stages can be turned on one after another to discharge the rainwater into the Huangpu River and the Yangtze River. Figure 14 shows the whole water system and the distribution of sluices and pumps in Shanghai [78]. As shown in Figure 14, the pumping stations and sluice gates of the Huangpu River can be utilized to discharge the large volumes of rapidly pouring water and control the water level of the river to prevent pluvial flooding hazards. Nowadays, the existing sluices and pumps are mainly concentrated inside the Outer ring road. In the future, construction of sluices and pumps will be increased outside the Outer ring road. With the aforementioned facilities, the water storage capacity and rainwater drainage ability can be adjusted as follows: (i) Turn off the sluices between the rivers inside the Outer ring road and outside the Outer ring road when the tide of the Huangpu River lowers, while the sluices of the rivers in the urban area will be turned on in order to drain water into the Huangpu River and Yangtze River. This will keep the water level of the inland rivers in the urban area at a low level and reserve enough storage space before torrential rainfall. (ii) When the tides of the Huangpu River rise, the afflux sluices along the Huangpu River will be turned off to prevent the water from backflowing into the inland rivers. With the Sponge City, the pluvial flooding hazards can be reduced, and the security of the drinking water can be effectively ensured.

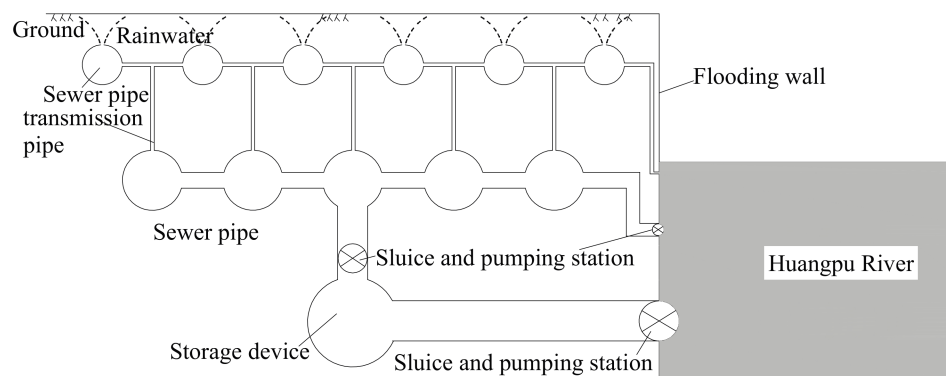


Figure 13. Schematic diagram of the Sponge City.

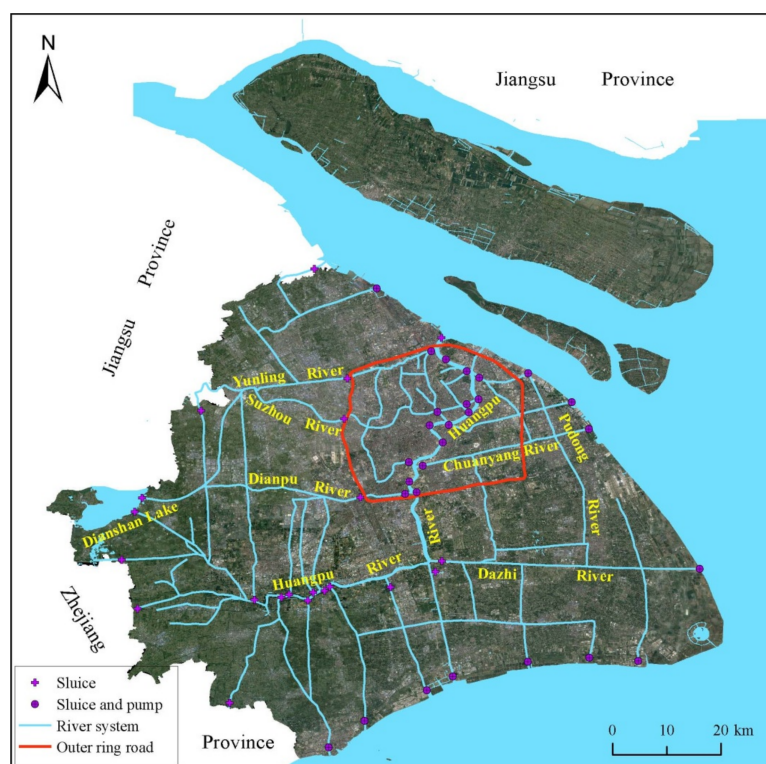


Figure 14. Whole water system and the distribution of sluices and pumps in Shanghai.

## 7. Conclusions

Heavy rainfall due to global warming and land subsidence poses a significant risk to coastal areas. The effect of global warming can be divided as follows: temperature variation and the regional sea level change; while the regional rate of sea level change in Shanghai can be divided into eustatic sea level change, tectonic movement of the continent and land subsidence of Shanghai. Because the average elevation of Shanghai ranges from 2.2 m to 4.5 m, it is imperative to reduce pluvial flooding hazards due to heavy rainfall, which is induced by global warming and land subsidence. In this paper, the correlation between heavy rainfall and global warming in Shanghai was analysed. Based on the analysis, the following conclusions can be drawn:

1. The torrential rainfall is concentrated from May to September. In recent years, extraordinary torrential rainfall and short duration rainfall showed an increasing trend, while the totals of torrential rainfall have remained about the same. Torrential rainfall parameters,  $P_m$  ranging from

50 mm to 150 mm, and  $I_a$  in the range of 5 mm/h to 60 mm/h, are more likely to induce pluvial flooding hazards.

2. Extraordinary torrential rainfall events and extraordinarily short duration torrential rainfall events easily lead to pluvial flooding hazards. With an increase in temperature, the frequency of extraordinarily short duration torrential rainfalls increases significantly, while the frequency of extraordinary torrential rainfalls increases somewhat with increases in sea level.
3. Pluvial flooding due to heavy rainfall may induce large potential damage to coastal structures and residents' lives. In recent years, the above hazards have become more serious. Thus, monitoring and database systems, with contemporary geomatics technologies such as GIS, GPS and RS should be used to effectively forecast heavy rainfall. Meanwhile, appropriate engineering treatment technology, such as repairing and increasing the capacity of the drainage system and the Sponge City, should be chosen for this type of hazard.

**Acknowledgments:** The research work described herein was funded by the National Nature Science Foundation of China (NSFC) (Grant No. 41472252). This financial support is gratefully acknowledged.

**Author Contributions:** Yao Yuan drafted the manuscript and constructed the figures; Ye-Shuang Xu collected the data and revised the manuscript; Arul Arulrajah checked the content and revised the manuscript. All authors made contributions to the study and the writing of the manuscript.

**Conflicts of Interest:** The authors declare no conflict of interest.

## References

1. Han, G.Q.; Huang, W.G. Pacific decadal oscillation and sea level variability in the Bohai, Yellow, and East China Sea. *J. Phys. Oceanogr.* **2008**, *38*, 2772–2783. [[CrossRef](#)]
2. Intergovernmental Panel on Climate Change (IPCC). *Climate Change 2014: Synthesis Report. Contribution of Working Groups I, II and III to the Fifth Assessment Report of the Intergovernmental Panel on Climate Change*; Core Writing Team, Pachauri, R.K., Meyer, L.A., Eds.; IPCC: Geneva, Switzerland, 2014; p. 151.
3. Ni, J.C.; Cheng, W.C. Field response of high speed rail box tunnel during horizontal grouting. *J. Test. Eval.* **2015**, *43*, 1–16. [[CrossRef](#)]
4. Shen, S.L.; Xu, Y.S. Numerical evaluation of land subsidence induced by groundwater pumping in Shanghai. *Can. Geotech. J.* **2011**, *48*, 1378–1392. [[CrossRef](#)]
5. Ni, J.C.; Cheng, W.C. Monitoring and modeling grout efficiency of lifting structure in soft clay. *Int. J. Geomech.* **2010**, *10*, 223–229. [[CrossRef](#)]
6. Shen, S.L.; Wu, H.N.; Cui, Y.J.; Yin, Z.Y. Long-term settlement behavior of the metro tunnel in Shanghai. *Tunn. Undergr. Space Technol.* **2014**, *40*, 309–323. [[CrossRef](#)]
7. Horpibulsuk, S.; Bergado, D.T.; Lorenzo, G.A. Compressibility of cement admixed clays at high water content. *Geotechnique* **2004**, *54*, 151–154. [[CrossRef](#)]
8. Horpibulsuk, S.; Rachan, R.; Suddepong, A.; Chinkulkijniwat, A. Strength development in cement admixed Bangkok clay: Laboratory and field investigations. *Soils Found.* **2011**, *51*, 239–251. [[CrossRef](#)]
9. Ma, L.; Xu, Y.S.; Shen, S.L.; Sun, W.J. Evaluation of the hydraulic conductivity of aquifer with piles. *Hydrogeol. J.* **2014**, *22*, 371–382. [[CrossRef](#)]
10. Du, Y.J.; Jiang, N.J.; Shen, S.L.; Jin, F. Experimental investigation of influence of acid rain on leaching and hydraulic characteristics of cement-based solidified/stabilized lead contaminated clay. *J. Hazard. Mater.* **2012**, *225–226*, 195–201. [[CrossRef](#)] [[PubMed](#)]
11. Yin, J.; Yin, Z.E.; Hu, X.M.; Xu, S.Y.; Wang, J.; Li, Z.H.; Zhong, H.D.; Gan, F.B. Multiple scenario analyses forecasting the confounding impacts of sea level rise and tides from storm induced coastal flooding in the city of Shanghai, China. *Environ. Earth Sci.* **2011**, *63*, 407–414. [[CrossRef](#)]
12. Shen, Q.Q.; Shu, J.; Wang, X.H. Multiple Time Scales Analysis of Temperature and Precipitation Variation in Shanghai for the Recent 136 Year. *J. Nat. Resour.* **2011**, *26*, 644–654. (In Chinese)
13. Yin, Z.Y.; Karstunen, M.; Chang, C.S.; Koskinen, M.; Lojander, M. Modeling time-dependent behavior of soft sensitive clay. *J. Geotech. Geoenviron. Eng.* **2011**, *137*, 1103–1113. [[CrossRef](#)]
14. Yin, Z.Y.; Xu, Q.; Hicher, P.Y. A simple critical state based double-yield-surface model for clay behavior under complex loading. *Acta Geotech.* **2013**, *8*, 509–523. [[CrossRef](#)]

15. Xu, Y.S.; Ma, L.; Du, Y.J.; Shen, S.L. Analysis of urbanization-induced land subsidence in Shanghai. *Nat. Hazards* **2012**, *63*, 1255–1267. [CrossRef]
16. Wu, H.N.; Shen, S.L.; Ma, L.; Yin, Z.Y.; Horpibulsuk, S. Evaluation of the strength increase of marine clay under staged embankment loading: A case study. *Mar. Georesour. Geotechnol.* **2015**, *33*, 532–541. [CrossRef]
17. Wu, H.N.; Shen, S.L.; Liao, S.M.; Yin, Z.Y. Longitudinal structural modelling of shield tunnels considering shearing dislocation between segmental rings. *Tunn. Undergr. Space Technol.* **2015**, *50*, 317–323. [CrossRef]
18. Yin, Z.Y.; Yin, J.H.; Huang, H.W. Rate-dependent and long-term yield stress and strength of soft Wenzhou marine clay: Experiments and modeling. *Mar. Georesour. Geotechnol.* **2015**, *33*, 79–91. [CrossRef]
19. Shen, S.L.; Ma, L.; Xu, Y.S.; Yin, Z.Y. Interpretation of increased deformation rate in aquifer IV due to groundwater pumping in Shanghai. *Can. Geotech. J.* **2013**, *50*, 1129–1142. [CrossRef]
20. Zhang, N.; Shen, S.L.; Wu, H.N.; Chai, J.C.; Yin, Z.Y. Evaluation of effect of basal geotextile reinforcement under embankment loading on soft marine deposits. *Geotext. Geomembr.* **2015**, *43*, 506–514. [CrossRef]
21. Wu, Y.X.; Shen, S.L.; Yuan, D.J. Characteristics of dewatering induced drawdown curve under barrier effect of retaining wall in aquifer. *J. Hydrol.* **2016**, *539*, 554–566. [CrossRef]
22. Wang, Z.F.; Shen, S.L.; Ho, E.C.; Kim, Y.H. Investigation of field installation effects of horizontal Twin-Jet grouting in Shanghai soft soil deposits. *Can. Geotech. J.* **2013**, *50*, 288–297. [CrossRef]
23. Wang, Z.F.; Shen, S.L.; Ho, C.E.; Xu, Y.S. Jet grouting for mitigation of installation disturbance. *Geotech. Eng. ICE Proc.* **2014**, *167*, 526–536. [CrossRef]
24. Shen, S.L.; Wang, Z.F.; Yang, J.; Ho, E.C. Generalized approach for prediction of jet grout column diameter. *J. Geotech. Geoenviron. Eng.* **2013**, *139*, 2060–2069. [CrossRef]
25. Wu, Y.X.; Shen, S.L.; Wu, H.N. Environmental protection using dewatering technology in a deep confined aquifer beneath a shallow aquifer. *Eng. Geol.* **2015**, *196*, 59–70. [CrossRef]
26. Du, Y.J.; Fan, R.D.; Reddy, K.R.; Liu, S.Y.; Yang, Y.L. Impacts of presence of lead contamination in clayey soil–calcium bentonite cutoff wall backfills. *Appl. Clay Sci.* **2015**, *108*, 111–122. [CrossRef]
27. Shen, S.L.; Wang, Z.F.; Sun, W.J.; Wang, L.B.; Horpibulsuk, S. A field trial of horizontal jet grouting using the composite-pipe method in the soft deposit of Shanghai. *Tunn. Undergr. Space Technol.* **2013**, *35*, 142–151. [CrossRef]
28. State Oceanic Administration, People's Republic of China (2000–2015). China Ocean Disasters Communique (CODC). Available online: <http://www.coi.gov.cn/gongbao/zaihai/> (accessed on 26 April 2017). (In Chinese)
29. Wei, Z.X.; Zhai, G.Y.; Yan, X.X. *Atlas of Shanghai Urban Geology*; Geology Press: Beijing, China, 2010.
30. Deng, J.L.; Shen, S.L.; Xu, Y.S. Investigation into pluvial flooding hazards caused by heavy rain and protection measures in Shanghai, China. *Nat. Hazards* **2016**, *83*, 1301–1320. [CrossRef]
31. State Oceanic Administration, People's Republic of China (2000–2015). China Ocean Bulletin (COB). Available online: <http://www.soa.gov.cn/zwgk/hygb/> (accessed on 26 April 2017). (In Chinese)
32. Wu, Y.X.; Shen, S.L.; Xu, Y.S.; Yin, Z.Y. Characteristics of groundwater seepage with cutoff wall in gravel aquifer. I: Field observations. *Can. Geotech. J.* **2015**, *52*, 1526–1538.
33. Shen, S.L.; Wang, J.P.; Wu, H.N.; Xu, Y.S.; Ye, G.L.; Yin, Z.Y. Evaluation of hydraulic conductivity for both marine and deltaic deposit based on piezocone test. *Ocean Eng.* **2015**, *110*, 174–182. [CrossRef]
34. Ni, J.C.; Cheng, W.C. Trial grouting under rigid pavement: A case history in Magong Airport, Penghu. *J. Test. Eval.* **2012**, *40*, 1–12.
35. Shen, S.L.; Wu, Y.X.; Xu, Y.S.; Hino, T.; Wu, H.N. Evaluation of hydraulic parameter based on groundwater pumping test of multi-aquifer system of Tianjin. *Comput. Geotech.* **2015**, *68*, 196–207. [CrossRef]
36. Cheng, W.C.; Ni, J.C.; Shen, S.L.; Huang, H.W. Investigation of factors affecting jacking force: A case study. *ICE Proc. Geotech. Eng.* **2017**. [CrossRef]
37. Cheng, W.C.; Ni, J.C.; Shen, S.L. Experimental and analytical modeling of shield segment under cyclic loading. *Int. J. Geomech. ASCE* **2017**, *17*, 04016146. [CrossRef]
38. Shen, S.L.; Cui, Q.L.; Ho, E.C. Ground response to multiple parallel micro tunneling operations in cemented silty clay and sand. *J. Geotech. Geoenviron. Eng.* **2016**, *142*, 1–11. [CrossRef]
39. Tan, Y.; Wang, D. Characteristics of a large-scale deep foundation pit excavated by the central-island technique in Shanghai soft clay. I: Bottom-up construction of the central cylindrical shaft. *J. Geotech. Geoenviron. Eng. ASCE* **2013**, *139*, 1875–1893. [CrossRef]



40. Tan, Y.; Wang, D. Characteristics of a large-scale deep foundation pit excavated by the central-island technique in Shanghai soft clay. II: Top-down construction of the peripheral rectangular pit. *J. Geotech. Geoenviron. Eng. ASCE* **2013**, *139*, 1894–1910. [[CrossRef](#)]
41. Tan, Y.; Li, X.; Kang, Z.; Liu, J.; Zhu, Y. Zoned excavation of an oversized pit close to an existing metro line in stiff clay: Case study. *J. Perform. Constr. Facil. ASCE* **2015**, *29*, 04014158. [[CrossRef](#)]
42. Tan, Y.; Huang, R.; Kang, Z.; Bin, W. Covered semi-top-down excavation of subway station surrounded by closely spaced buildings in downtown Shanghai: Building response. *J. Perform. Constr. Facil.* **2016**, *30*, 04016040. [[CrossRef](#)]
43. Yuan, Y.; Shen, S.L.; Wang, Z.F.; Wu, H.N. Automatic Pressure-Control Equipment for Horizontal Jet-grouting. *Autom. Constr.* **2016**, *69*, 11–20. [[CrossRef](#)]
44. Shen, S.L.; Wang, Z.F.; Cheng, W.C. Estimation of lateral displacement induced by jet grouting in clayey soils. *Geotechnique* **2017**. [[CrossRef](#)]
45. Zhang, J.; Lin, Z. *Climate of China*; John Wiley & Sons: New York, NY, USA, 1992; p. 376.
46. He, F.F.; Zhao, B.K. The characteristics of climate change of torrential rains in Shanghai region in recent 30 years. *Adv. Earth Sci.* **2009**, *24*, 1260–1267.
47. He, F.F. Characteristics of torrential rain in Shanghai from 1980s. In Proceedings of the Urban Meteorology Forum—Urban and Climate Change, Shenzhen, China, 24–25 November 2012; pp. 10–17. (In Chinese)
48. Cao, A.L.; Zhang, H.; Zhang, Y.; Ma, W.C. Decadal changes of air temperature in Shanghai in recent 50 years and its relation to urbanization. *Chin. J. Geophys.* **2008**, *51*, 1663–1669. (In Chinese)
49. Shanghai Statistical Yearbook (SSY). *Shanghai Municipal Bureau of Statistics*; China Statistics Press: Shanghai, China, 2001–2015. (In Chinese)
50. Bindoff, N.L.; Willebrand, J.; Artale, V.; Cazenave, A.; Gregory, J.; Gulev, S.; Hanawa, K.; Le Quéré, C.; Levitus, S.; Nojiri, Y.; et al. Observations: Oceanic Climate Change and Sea Level. In *Climate Change 2007: The Physical Science Basis. Contribution of Working Group I to the Fourth Assessment Report of the Intergovernmental Panel on Climate Change*; Solomon, S., Qin, D., Manning, M., Chen, Z., Marquis, M., Averyt, K.B., Tignor, M., Miller, H.L., Eds.; Cambridge University Press: Cambridge, UK; New York, NY, USA, 2007; Volume 996, pp. 408–419.
51. Liu, X.Y.; Liu, Y.G.; Guo, L.; Rong, Z.R.; Gu, Y.Z.; Liu, Y.H. Interannual changes of sea level in the two regions of East China Sea and different responses to ENSO. *Glob. Planet. Chang.* **2010**, *72*, 215–226. [[CrossRef](#)]
52. Nerem, R.S.; Éric, L.; Cazenave, A. Present-day sea-level change: A review. *C. R. Geosci.* **2006**, *338*, 1077–1083. [[CrossRef](#)]
53. Church, J.A.; Gregory, J.M.; Huybrechts, P.; Kuhn, M.; Lambeck, K.; Nhuan, M.T.; Qin, D.; Woodworth, P.L. *Changes in Sea Level, in Intergovernmental Panel on Climate Change, Third Assessment Report*; Cambridge University Press: New York, NY, USA, 2001; pp. 639–694.
54. Chambers, D.P.; Ries, J.C.; Urban, T.J. Calibration and verification of Jason-1 using global along-track residuals with TOPEX. *Mar. Geod.* **2003**, *26*, 305–317. [[CrossRef](#)]
55. Wei, Z.X.; Gong, S.L. Sea level rising and it's possible impacts on Shanghai in future. *Shanghai Geol.* **1998**, *65*, 14–20. (In Chinese)
56. Zhang, H.; Li, Q.F.; Yu, M.X.; Ren, J.L.; Li, P.C. Frequency Analysis of Annual Maximum Tide Level in Huangpu River in Times of Intense Change. *Water Resour. Power* **2014**, *32*, 1–5. (In Chinese)
57. Zhang, A.G.; Wei, Z.X. *Land Subsidence in China*; Shanghai Scientific and Technical Publishers: Shanghai, China, 2005. (In Chinese)
58. Tian, B.; Zhang, L.; Wang, X.; Zhou, Y.; Zhang, W. Forecasting the effects of sea-level rise at Chongming Dongtan Nature Reserve in the Yangtze Delta, Shanghai, China. *Ecol. Eng.* **2010**, *36*, 1383–1388. [[CrossRef](#)]
59. Lyu, H.M.; Wang, G.F.; Shen, J.S.; Lu, L.H.; Wang, G.Q. Analysis and GIS mapping of flooding hazards on 10 May, 2016, Guangzhou, China. *Water* **2016**, *8*, 447. [[CrossRef](#)]
60. Lyu, H.M.; Wang, G.F.; Cheng, W.C.; Shen, S.L. Tornado hazards on June 23rd in Jiangsu Province, China: Preliminary investigation and analysis. *Nat. Hazards* **2017**, *85*, 597–604. [[CrossRef](#)]
61. Gong, Y.W.; Liang, X.Y.; Li, X.N.; Li, J.Q.; Fang, X.; Song, R.N. Influence of rainfall characteristics on total suspended solids in urban runoff: A case study in Beijing, China. *Water* **2016**, *8*, 278. [[CrossRef](#)]
62. Wang, Y. Advances in remote sensing of flooding. *Water* **2015**, *7*, 6404–6410. [[CrossRef](#)]
63. Zhu, Q.G.; Lin, J.R.; Shou, S.W.; Tang, D.S. *Principles and Methods of Synoptic Meteorology*; China Meteorological Press: Beijing, China, 2007.

64. Simões, N.E.; Ochoa-Rodríguez, S.; Wang, L.P.; Pina, R.D.; Marques, A.S.; Onof, C.; Leitão, J.P. Stochastic urban pluvial flood hazard maps based upon a spatial-temporal rainfall generator. *Water* **2015**, *7*, 3396–3406. [CrossRef]
65. Qing, S.; Zhang, Y.S.; Hu, E.H.; Lu, C.H. Potential impacts of sea level rise on the economy and environment in the Yangtze River delta and the countermeasures thereof. *Resour. Environ. Yangtze Val.* **1997**, *6*, 58–64. (In Chinese)
66. Yan, B.; Li, S.; Wang, J.; Ge, Z.M.; Zhang, L.Q. Socio-economic vulnerability of the megacity of Shanghai (China) to sea-level rise and associated storm surges. *Reg. Environ. Chang.* **2015**, *16*, 1443–1456. [CrossRef]
67. China Meteorological Administration. Available online: [http://www.cma.gov.cn/2011xzt/2013zhuan/20130720/2013072001/201307/t20130719\\_220272.html](http://www.cma.gov.cn/2011xzt/2013zhuan/20130720/2013072001/201307/t20130719_220272.html) (accessed on 26 April 2017).
68. Cao, X.G.; Zhang, J.; Wang, H.; Chen, Y.L. Analysis on a Severe Convective rainstorm hitting Shanghai on 25 August 2008. *Meteorol. Mon.* **2009**, *35*, 51–58. (In Chinese)
69. Fang, G.L.; Xie, Y.Y.; Li, Y.P.; Li, D.M. Research on the early warning system for rainstorm waterlogging in Shanghai city. *Atmos. Sci. Res. Appl.* **2009**, *2*, 32–41. (In Chinese)
70. Zhang, W.; Che, W.; Wang, J.L.; Wang, S.S. Management of urban stormwater runoff by green Infrastructures. *China Water Wastewater* **2011**, *27*, 22–27.
71. Xu, H.S.; Zhang, Q.Z.; Cai, Y.L. Hydrological Simulation of Rainfall Runoff Based on the View of Stormwater Integrated Management in Shanghai Lingang New City. *Geogr. Geo-Inf. Sci.* **2013**, *3*, 026.
72. Du, Y.J.; Jiang, N.J.; Liu, S.Y.; Jin, F.; Singh, D.N.; Puppala, A.J. Engineering properties and microstructural characteristics of cement-stabilized zinc-contaminated kaolin. *Can. Geotech. J.* **2014**, *51*, 289–302. [CrossRef]
73. Du, Y.J.; Wei, M.L.; Reddy, K.R.; Liu, Z.P.; Jin, F. Effect of acid rain pH on leaching behavior of cement stabilized lead-contaminated soil. *J. Hazard. Mater.* **2014**, *271*, 131–140. [CrossRef] [PubMed]
74. Horpibulsuk, S.; Rachan, R.; Chinkulkijniwat, A.; Raksachon, Y.; Suddepong, A. Analysis of strength development in cement-stabilized silty clay based on microstructural considerations. *Constr. Build. Mater.* **2010**, *24*, 2011–2021. [CrossRef]
75. Cheng, J.; Yang, K.; Zhao, Y.; Yuan, W.; Wu, J.P. Variation of River System in Center District of Shanghai and Its Impact Factors During the Last One Hundred Years. *Sci. Geogr. Sin.* **2007**, *27*, 85–91. (In Chinese)
76. Li, X.N.; Li, J.Q.; Fang, X.; Gong, Y. Case Studies of the Sponge City Program in China. In Proceedings of the World Environmental and Water Resources Congress, West Palm Beach, FL, USA, 22–26 May 2016; pp. 295–308.
77. Xu, Y.S.; Shen, S.L.; Ren, D.J.; Wu, H.N. Factor analysis of land subsidence in Shanghai: A view based on Strategic Environmental Assessment. *Sustainability* **2016**, *8*, 573. [CrossRef]
78. Dai, S.Z. Research on the planning and construction strategy of sponge city in Shanghai. *Shanghai Urban Plan. Rev.* **2016**, *1*, 9–12. (In Chinese)

